RIDGE SYSTEMS RELATED TO MARTIAN IMPACT CRATERS

J. RAITALA and K. KAUHANEN

Department of Astronomy, University of Oulu, Finland

(Received 4 March 1992)

Abstract. Wrinkle ridge systems within and around Martian highland craters were studied in order to find their basin-induced and regional aspects. Most prominent ridge directions indicate regional tectonic patterns. Radial ridges near large craters are often slightly deflected along regional or global ridge systems. Crater floor ridges have simpler local distributions. Smaller or older craters are less resistant against the effects of global or regional stress systems. In craters concentric ridge rings locate at 0.8 crater radius with additional minor rings at 0.66, 0.44 and 0.94 crater radius. This pattern illustrates compression of lava fill over buried topography.

1. Introduction

Ridges within and near impact basins exhibit tectonic patterns of basin-induced, regional and global stresses. These stresses are primarily caused by gravitational settling of the basin and local or global extension and compression (Maxwell, 1978). Arcuate ridges on borders of circular lunar maria are explained by the subsidence control of the basalt-loaded basin interior. Complex linear patterns relate to regional volcanic, tectonic or global stress systems.

Wrinkle ridges on Mars occur on all types of terrain including smooth plains and heavily cratered highland areas (Chicarro and Schultz, 1982). Most of the Martian ridges may be controlled by regional compressional stresses due to volcanic loads or ancient impact basins (Chicarro, Schultz and Masson, 1983). The absence of tensional features around ridged plains indicates that basic cause of the compression was an areal contraction of Martian interiors rather than a mere surface load (Raitala, 1987).

Basin-controlled ridge systems have been identified within and nearby over 30 impact basins on Mars (Chicarro and Schultz, 1983; Chicarro and Schultz, 1985). Most basins have multiple rings or knobby remnants of them around. The inter-ring area shows a more concentric pattern particularly in the shallower parts of a basin (Raitala, 1987). Pronounced concentric or radial ridges are found outside the basin ring as far as one basin diameter from the center (Chicarro and Schultz, 1983). In the case of multiple rings, ridges often concentrate on plains between adjacent rings. If local regional and basin-related ridges are omitted, a major residual ridge and scarp system emerges (Chicarro and Schultz, 1983). While the global grid is not identifiable, this system may indicate effects of some large-scale forces.

Earth, Moon, and Planets **58**: 65–78, 1992.

TABLE I

Studied basins

Basin	Location	Diam. (km)	Main ridge direction	
			Dominant	Other
Maggini area				
Maggini	Arabia NW	140	N35° W	N55° W
Arabia. Nx	Arabia NW	80	N5° W	
Schiaparelli area				
Schiaparelli	Sinus Sabaeus NW	460	N40° W	N10° W, N10° E
Flaugergues	Sinus Sabaeus SW	220	N30° W	N5° E
Wislicenus	Sinus Sabaeus SW	140	N35° W	N5° E
Denning	Sinus Sabaeus SE	150	N15° E	N65° W
Bouguer	Sinus Sabaeus SE	100	N45° W	
Antoniadi area				
Cassini	Arabia NE	430	N15° W	N45° W, N25° E
Tikhonravov	Arabia SE	150	N15° W	
Flammarion	Syrtis Major NW	170	N35° W	N5° W
Schöner	Syrtis Major NW	215	not measured	
Antoniadi	Syrtis Major NW	390	N35° W	N5° W
Huygens area				
Schroeter	Iapygia NW	280	N40° E	N5° E, N45° W
Huygens	Iapygia NW	470	N40° E	N55° W, N75° E
Herschel area				
Herschel	Mare Tyrrhenum NW	285	N70° W	N15° W
Aeolis.Wn	Aeolis SW	75	N65° W	N15° W
Aeolis. 1	Aeolis SW	80	N65° W	N20° W, N65° E
Graff	Aeolis SW	140	N5° W	N25° W, N45° W
Molesworth	Aeolis SW	175	N5° W	N45° W

2. Areas and Object of the Study

In order to investigate the role of basin-induced stresses in ridge formation we have measured length and orientation of wrinkle ridges in the vicinity of some impact craters on Martian highland (Table I). Comparing ridge directions and abundance within and outside a crater one can find out which directions were part of a large-scale shortening of the crust and which directions were affected or caused by basin-induced stresses. Craters with inside or outside ridges were selected for the study. Subareas were chosen according to distinguished ridge orientation and/or geological unit (Figure 1). Measurements were made over five large areas on Martian highland.

3. Areal Studies

3.1 Maggini area

The area consists of two small craters surrounded by several sparsely ridged plains larger than the craters. Three separate trends can be discerned. A few ridges inside Maggini (Figure 2) are consistent with a general northwestern pattern which

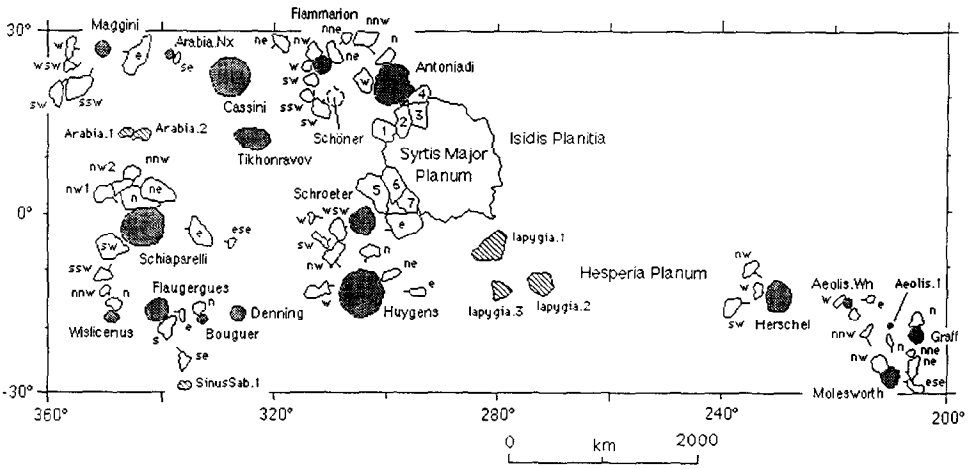

Fig. 1. Index map of the areas studied. The main craters of interest are indicated with grey patterns. Closely studied subareas, named after the closest main crater, are indicated by a barb pointing to the crater and a code specifying the direction of the subarea viewed from the main crater.

is also visible in most of the subareas and extends over a wide area of Schiaparelli and Antoniadi. The southern and eastern subareas represent a strikingly different regional trend of N25° E. Some north trending ridges can be seen in western and eastern subareas. The crater Arabia Nx (Figure 2) has no particular ridge pattern.

Ridges near Maggini are scattered and no one of the three directions is dominating. The northwestern trend present inside the crater cannot be explained by a mere local force because it remains similar over a wide area. It shows rather a wide areal tectonics of Martian surface after the formation of the craters. This leads also to the assumption that the crater wall is filtering out some of regional forces. However, Arabia Nx (Figure 2) seems to have all ridge directions.

3.2. Schiaparelli area

Schiaparelli (Figure 3) has a well defined linear ridge patterns on the eastern half of the basin. The first one of the three main components (N45° W, N15° W and N10° E) seems to be consistent with the orientation of stress trajectories from Tharsis (Maxwell and Gifford, 1981). In places a 34 km spacing of main ridges is seen. Concentric patterns can be weakly seen near the basin rim. The obvious lack of concentric ridges can be explained with thick mantling of the crater floor.

Surface markings of a former impact ring can be seen south of Schiaparelli. Areas just north of the basin show evidence of thick mantling (ridge rings), and this may be related to locally induced volcanism by former impacts. The main ridge direction N45° W is strongest in the northern subarea (Figure 3) and it gradually disappears to the north. The direction of this peak seems to have minor variations. Another main direction N15° W is present also in the southern subareas (Figure 3) and may indicate a broader pattern. The N10° E peak has its only

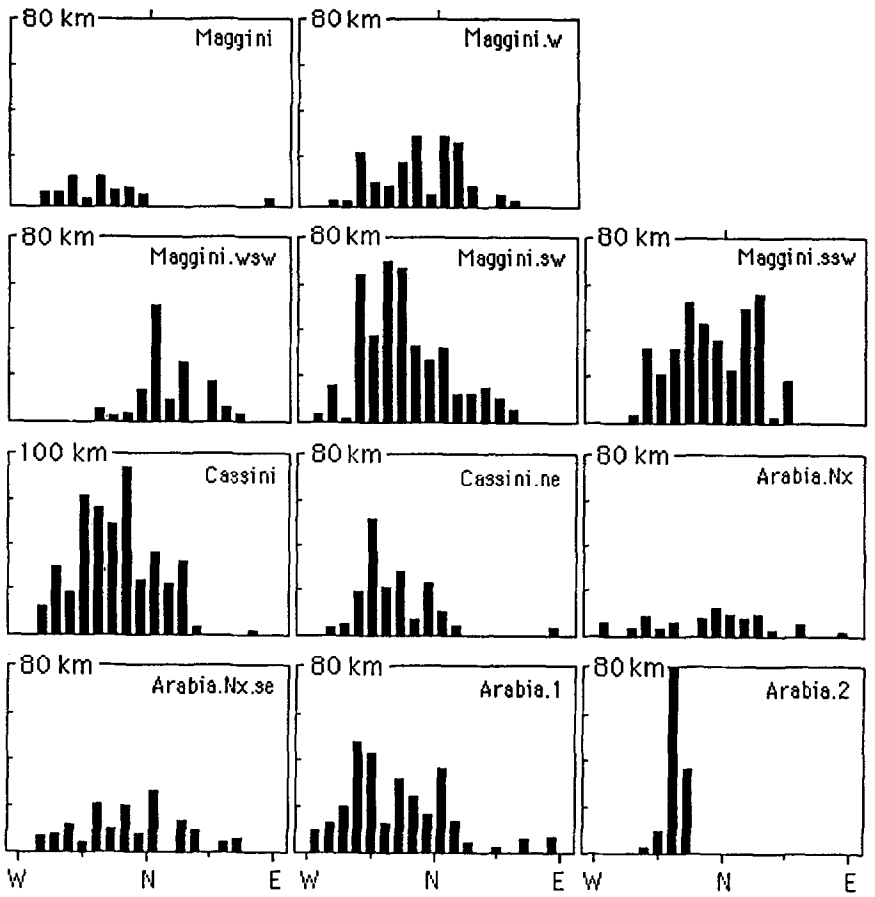

Fig. 2. The orientation distribution of ridges in the Maggini area. The vertical cumulative ridge length for each histogram is indicated in the upper left corner.

occurrences in NNW and SW of Schiaparelli and north of Wislicenus and may represent a distinct but minor regional pattern.

Two peaks arise from the data of Flaugergues (Figure 3). A strong northwestern (N30° W) pattern is similar to regional system of scarps in the same area (Maxwell and Gifford, 1981). Close to the western side of the crater rim the pattern is deflected to form a subconcentric pattern. Additional north-trending ridges are found in the crater. This orientation is also found in Schiaparelli, Wislicenus, Denning and in most of the intercrater areas (Figure 3). Ridges around Flaugergues show similar patterns as on the bottom of the crater. North-trending pattern is slightly stronger and northwestern pattern somewhat weaker. No major peaks are seen.

A faint set of ridges oriented N75° W can be seen in most of the areas around Schiaparelli. It is best displayed east of the basin but can be found also around Flaugergues.

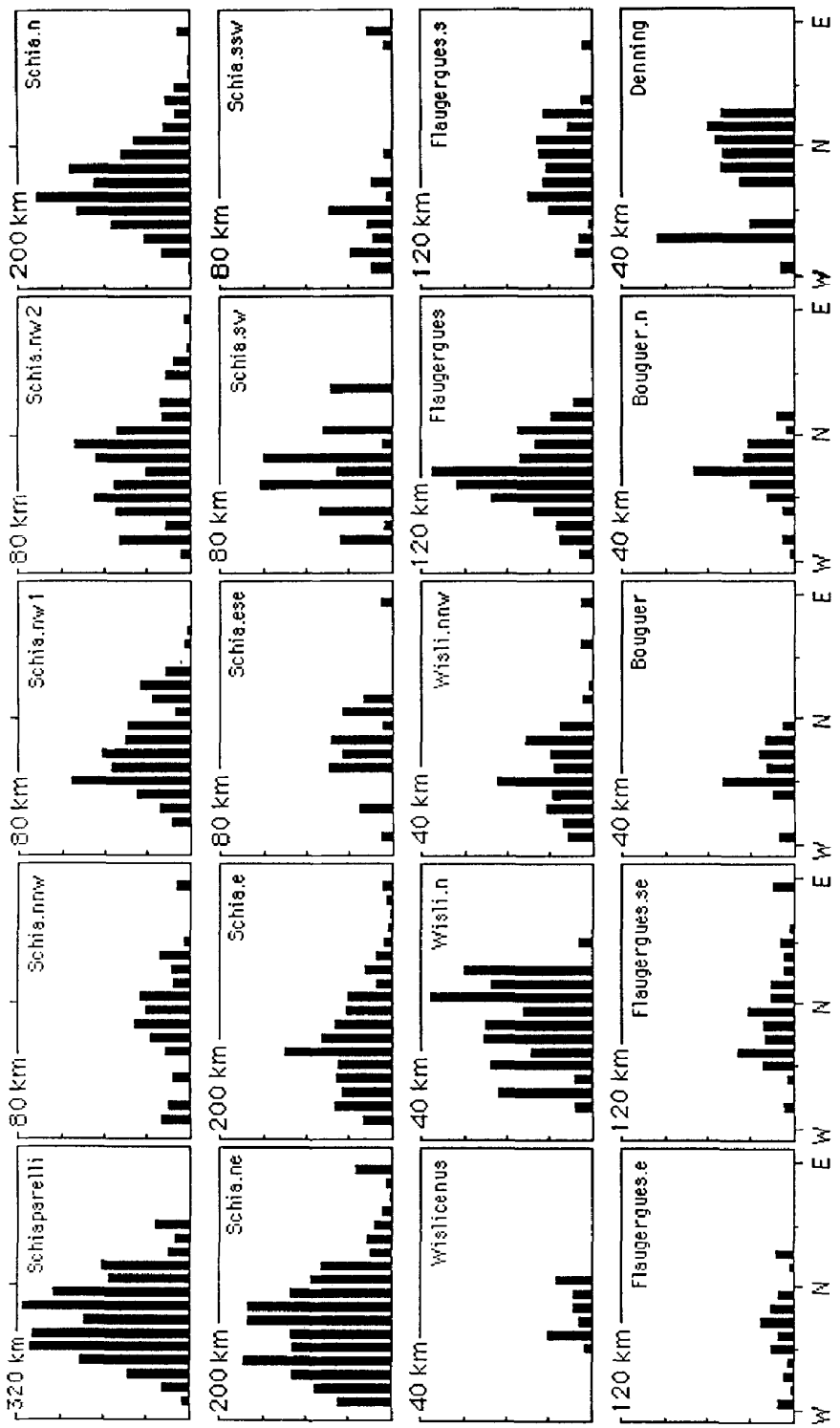

Fig. 3. The orientation of ridges in the Schiaparelli area.

3.3. Antoniadi area

The floor of Cassini is rough and the crater rim is partially degraded. Remnants of inner ring structure can be found. Histogram of the ridges (Figure 4) shows numerous peaks (N15° W, N45° W, N25° E). A regional scarp system has the orientation of N30° W, which seems to be inconsistent with the ridge directions. Most ridges which are clearly visible in the center of the crater do not match with any regional pattern. The N15° W peak is also present in Tikhonravov and the Schiaparelli area and it is a broader-scale regional or global pattern.

Antoniadi is close to Syrtis Major Planum and is partly filled with lavas from vents on the northern flank of the planum. Its rim is very degraded. Ridge directions present trends similar to the ridges on the northern flanks of Syrtis Major volcanic shield. Ridges are scattered on the crater floor and may thus be just a continuation of the ridges on Syrtis Major. The crater rim does not change ridge directions. North of Antoniadi there are two areas that indicate a clear NE–SE trend. Further on, third area has a strikingly different NE–SW pattern, although the main NE–SE trend remains (Figure 4).

Flammarion has a distinct NE–SE ridge pattern, although there are some ridges oriented N15 °W. Just outside the crater, a N10 °E ridge pattern is faintly visible. This pattern, as well as almost similar pattern in the northernmost area of Antoniadi can be referred to as ridges concentric to the Isidis basin.

Regional fault system near Antoniadi and Flammarion affects the histograms. Phison Rupes is oriented N30° W and most of the areas have a peak between N20° W–N50° W (Figure 4). Although the peak is slightly offset from place to place, a regional stress pattern can be inferred. Another peak (N5° W) can be joined with the north trending ridges of Syrtis Major Planum and also of Cassini and Schiaparelli.

3.4. Huygens area

Huygens contains a well developed concentric pattern of ridges, which approximately lie on an inner circular ring. This can be explained with total but shallow filling of the crater bottom. Central parts of the crater show distinct linear patterns oriented N40° E, N55° W and N75° E (Figure 5). These are consistent with regional scarps, ridges and grabens around the crater. The tectonics of nearby Syrtis Major Planum and Isidis Planitia have affected in producing a diversity of ridge directions inside the crater.

Around Huygens there is strong evidence of a radial pattern of ridges that has slightly deflected along the regional ridge patterns (Figure 5). Radial stresses of the former impact event may have controlled the crustal zones of weakness and thus partly guided the ridge formation. The elongated lava areas are also roughly radial to the crater and their form may have controlled ridges.

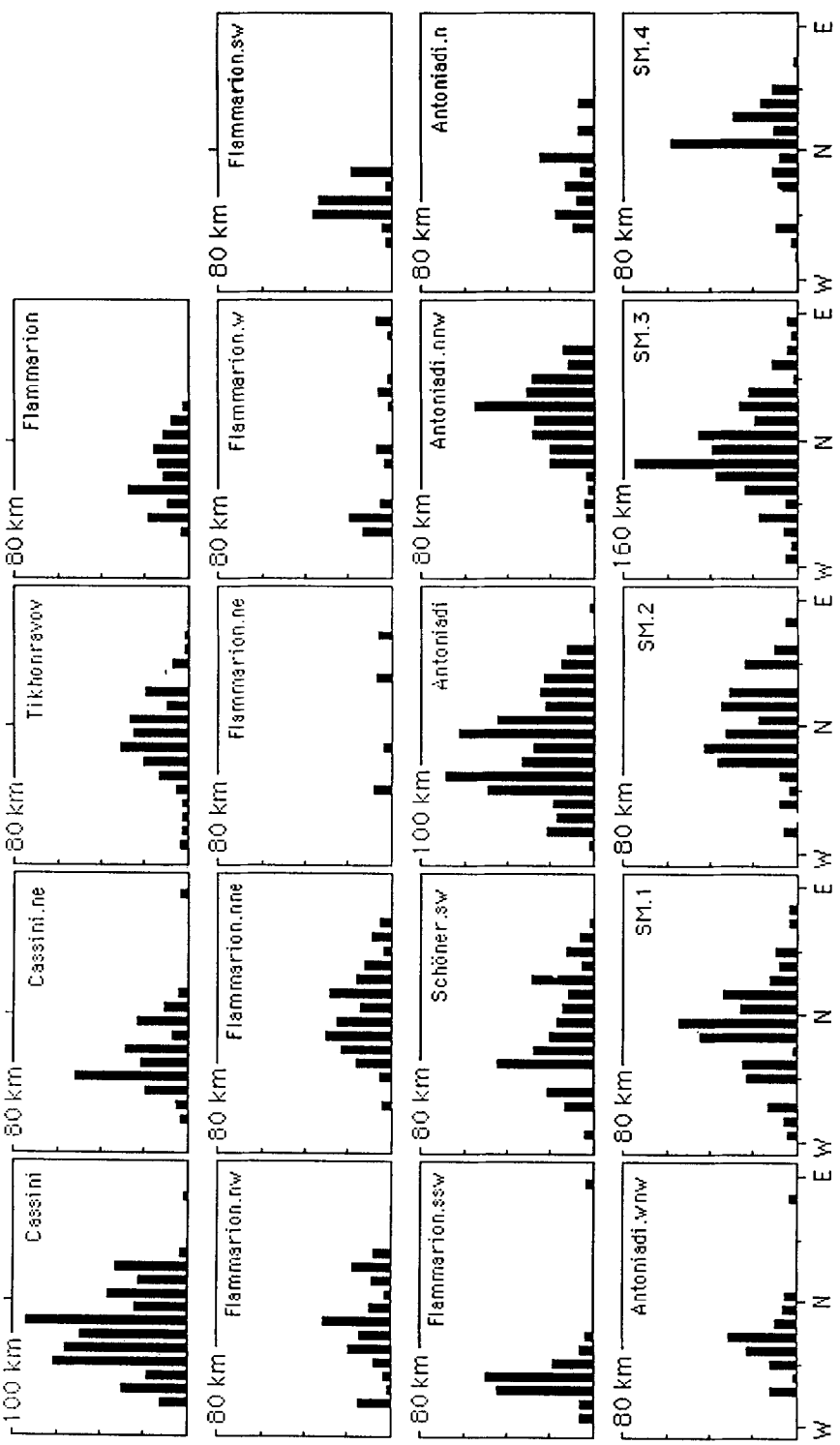

Fig. 4. The orientation of ridges in the Antoniadi area.

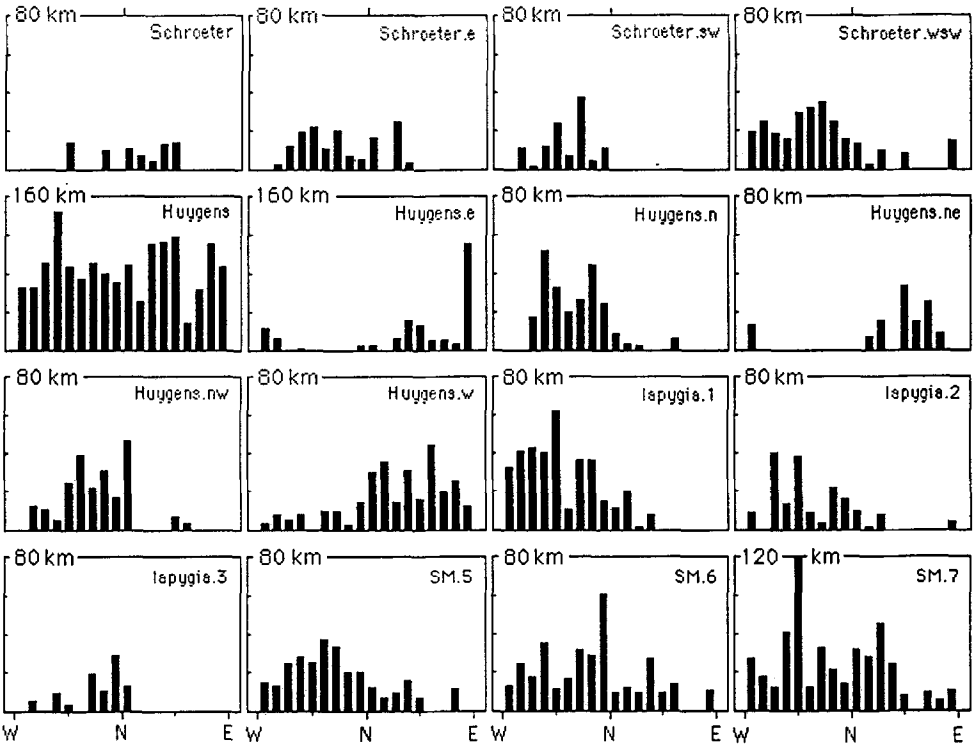

Fig. 5. The orientation of ridges in the Huygens area.

3.5. Herschel Area

Herschel shows a rather clear WNW pattern of ridges on the northern half of the basin. There seems to be no concentric ridges either in or outside the basin. Outside the Herschel basin several ridge directions in addition to the WNW trend can be found. The most distinct of them are N10° E and N30° W. (Figure 6).

There are also a few smaller craters on this area. A NW–SE trend is found on almost every measured area. Generally, subareas exhibit similar patterns as the crater bottoms. A N70° W pattern is found in the subareas of Molesworth. This trend becomes stronger to the northwest. To the east of Molesworth there is a totally different peak in the histograms, N20° E. As a conclusion, craters on this area are too old or too small to resist even faint regional stresses intruding the crater.

4. Ridges on Basin Floors

While extensional features are seen in the intercrater areas particularly close to Syrtis Major Planum, all measured basins show evidence of compressional tectonics. The age of the craters and thus the amount of erosion varies significantly. The intensity of compression can be approximated by cumulative ridge length. It is a

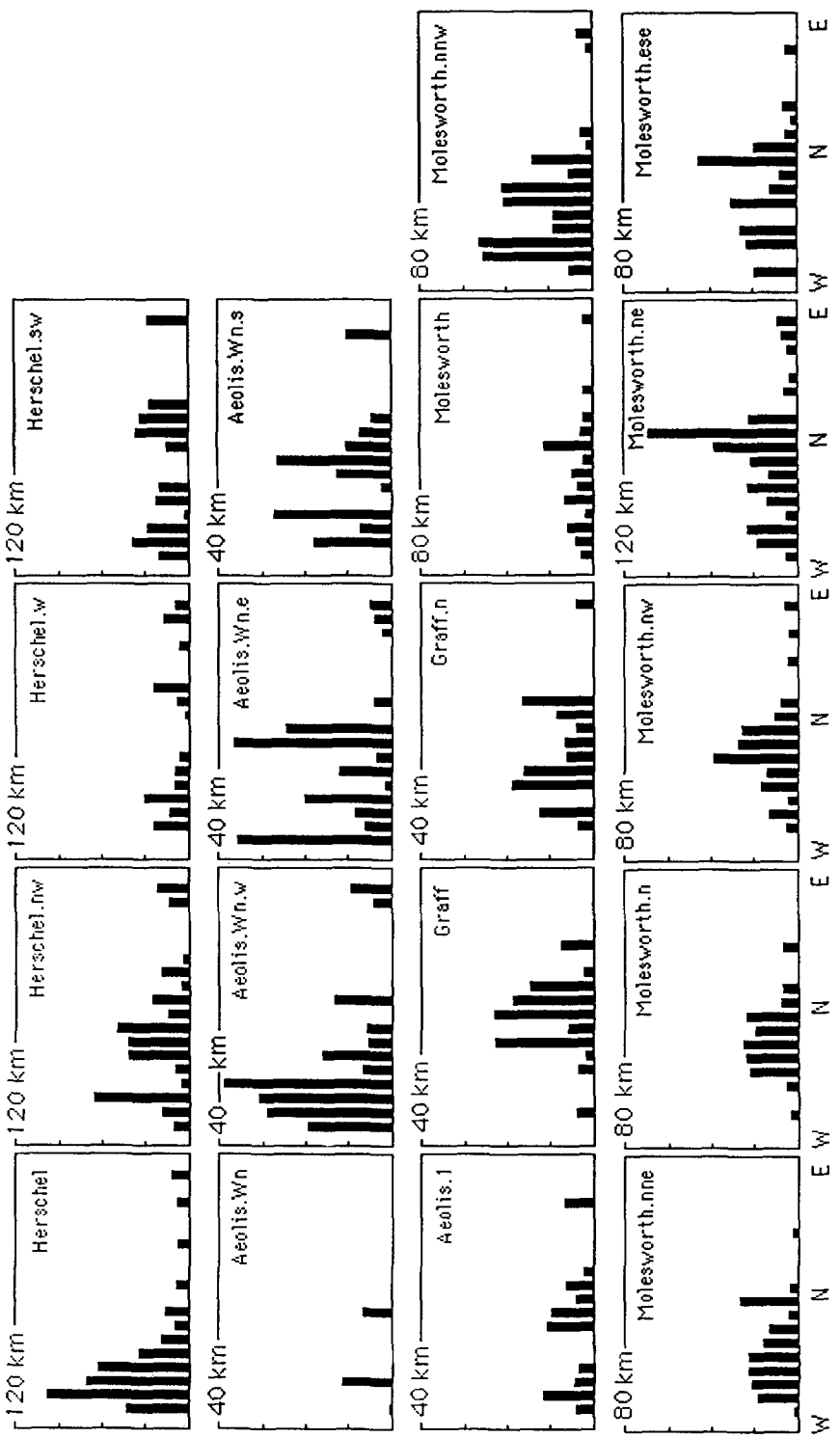

Fig. 6. The orientation of ridges in the Herschel area.

function of basin diameter only on a coarse level (Figure 7a) and may be more important in larger craters. The increasing amount of ridges with increasing basin diameter could be explained by a fact that a larger basin can hold more ridges. Ridges are, however, not evenly distributed and comparing the density of ridges to the basin diameter, no correlation can be found.

Differences between the orientations of ridges outside and in a crater may be caused by age difference between the impact crater and the surrounding terrain. The strength and broadness of the compressional forces may play an important role. Crater rim, if not heavily degraded, can prevent faint forces from intruding inside the crater.

Concentric ridges were found on crater floors where the bottom was filled. A correlation between the distance of the maximum of concentric ridges (Figure 8) and the crater diameter was found (Figure 7b, c). Distance measured from the crater rim seemed to be more dependent on the crater diameter. Concentric ridge locations compared with the scaled crater radius gave approximately the same value (0.8 radius) in every studied crater while there were also additional peaks at 0.66 radius, 0.44 radius and 0.94 radius (Figure 9).

5. Conclusions

In general, ridges on crater floors are simpler and only the strongest global and areal patterns are seen in craters. Within smaller or older craters, weak or degraded rim structure is less resistant against the effects of global or regional stress systems, particularly if they are strong (Maxwell and Gifford, 1981). Large deviations in the amount of clearly basin-induced ridges within large basins can be explained with the thickness of fill (Maxwell and Gifford, 1981). Regional patterns obscure the basin-related patterns on deeply flooded crater floors. Therefore, basin related ridges are mostly found near the crater rim on deeply filled craters.

The age or degradation of a crater can be seen in the diversity of ridges inside the crater. On the eastern side of Syrtis Major, ridges inside small craters have one clear direction. This may indicate the effect of a large regional to global force. The crater rim has prevented minor forces from intruding inside the crater. Near Herschel small craters do not have a main ridge direction of their own but only similar ridge directions than areas outside the craters.

All craters have a different kind of orientation histogram because of different regional and basin-induced tectonics. Areas that include more ridges show more continuous histograms of Gaussian form. Prominent peaks or sudden steps indicate intruding regional patterns. The distribution of ridges is thus not always that of Gaussian form and it does not cover all directions. Ridges may cover only a limited area of the basin floor near the rim, where the thickness of fill is shallower.

The N45° W orientation is found on most craters and subareas. It seems to be strongest near and inside Schiaparelli. Crater floors exhibit more homogeneous

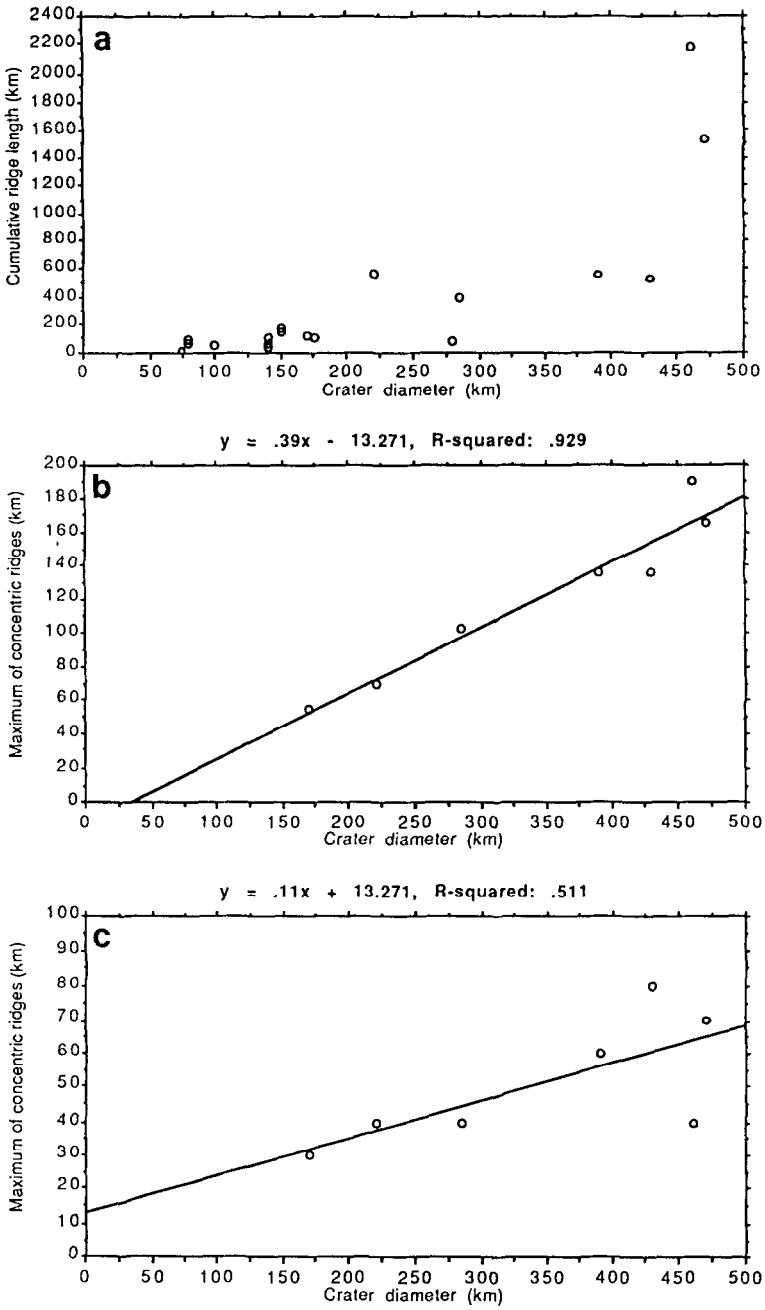

Fig. 7. Cumulative ridge length versus crater diameter for the selected basins (a). Distance of concentric ridge maximum (cf. Figure 9) measured from the crater rim (b) and from the crater centre (c). Concentric ridges heavily relate to the crater rim.

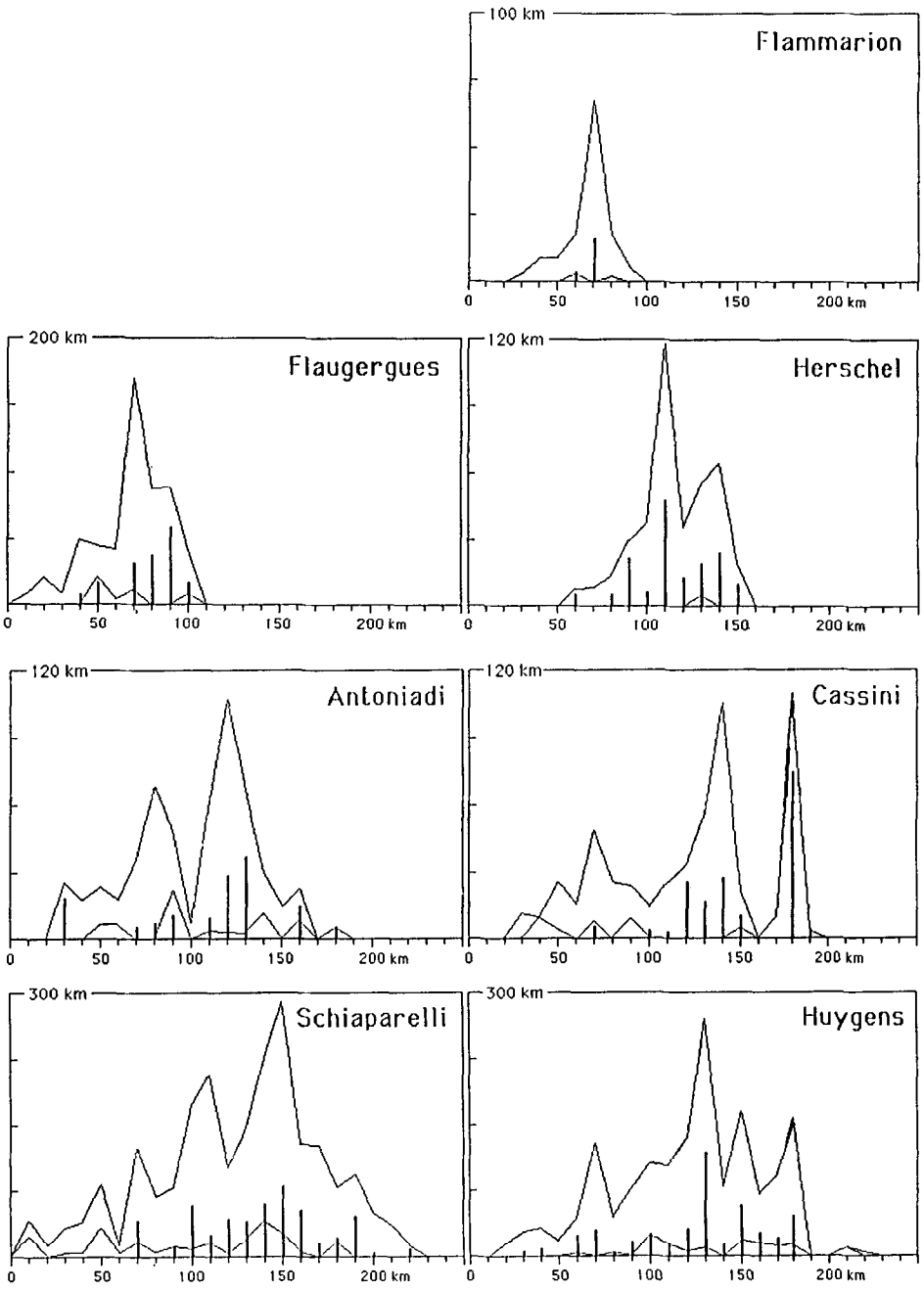

Fig. 8. Distance of concentric ridges measured from the crater centre compared with crater radius for some Martian craters. For each diagram the uppermost line represents the total length of all ridges at certain distances from the crater centre, lower line represents that of radial ridges and bars indicate locations and total lengths of concentric ridges.

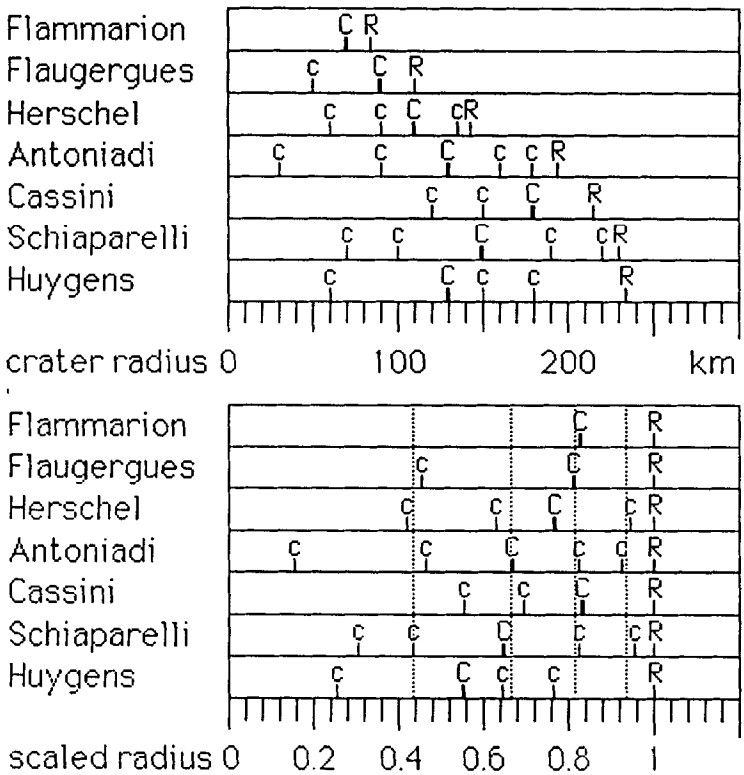

Fig. 9. Distances of concentric ridges (C,c) from the crater centre compared with the (scaled; lower part) crater radius (R) for some Martian craters. The upper case C indicates the location of the main peak taken from Figure 8 while the lower case c marks the locations of the additional peaks. There is a concentration of concentric mare ridges at 0.8 R with additional concentrations at 0.66 R, 0.44 R and 0.94 R indicating influences of crater-related stresses to the mare ridge formation within crater interiors.

distributions of ridge directions than the adjacent areas. Linear ridge direction on the crater floor may continue outside the crater. Areas within one crater diameter usually show some similarities to the crater itself. The most distinct peak may then disappear outside the crater and new peaks arise from the data.

Ridges inside and near small (<100 km) craters seem to behave like those connected to the larger ones. The main regional peak disappears and other more local peaks arise inside the crater rim. This, however may be due to insufficient data and there are some areal differences.

Concentric ridges can be found on older craters, which are filled with lava or aeolian material. They appear near the crater rim or along an inner circle. The majority of concentric ridges lie on an inner ring closest to the crater rim (Figure 9). Obviously the crater floor fill has broken under compression where it was thinnest (Figure 10). There are slight deviations in the pattern.

Concentric ridges inside the crater display effects of stress on the crater floor fill. In deeply filled craters there are weaker concentric patterns. The distance of

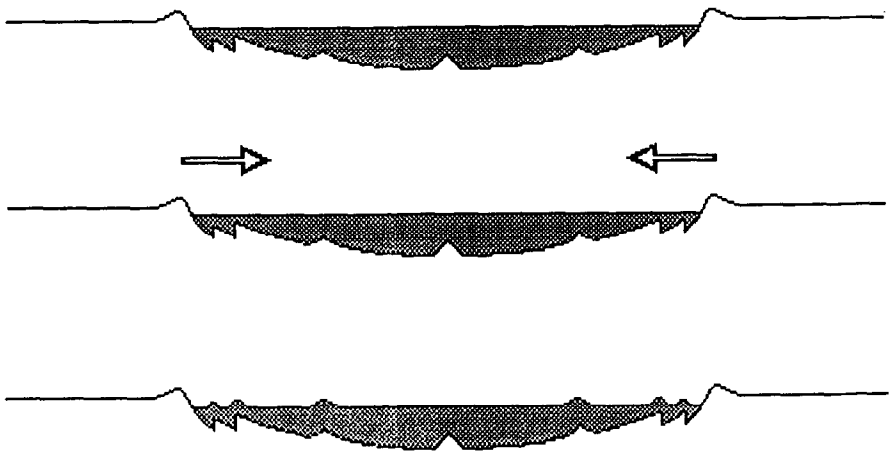

Fig. 10. A simple model for the development of ridges on a lava filled crater floor.

concentric ridges to the crater rim is dependent of the crater diameter. Concentric ridges were found at 0.8, 0.66, 0.44 and 0.94 crater radius. This indicates influences of buried topography and radial crater-related stresses in the mare ridge formation within crater interiors (Figures 8, 9, 10). Deviations of the pattern can be explained with variations in buried topography and filling of the crater floor.

Radial ridges found near larger craters indicate effects of radial stresses due to a large impact explosion. Such ridges are often slightly deflected along regional or global ridge systems.

References

Chicarro, A. F. and Schultz, P. H.: 1982, *Lunar Planet. Sci.* **XIII**, 88–89.
Chicarro, A. F. and Schultz, P. H.: 1983, *Lunar Planet. Sci.* **XIV**, 146–147.
Chicarro, A. F. and Schultz, P. H.: 1985, *Icarus* **63**, 153–174.
Chicarro, A. F., Schultz, P. H., and Masson, P.: 1983, *Lunar Planet. Sci.* **XIV**, 105–106.
Maxwell, T. A.: 1978, *Lunar Planet. Sci.* **IX**, 3541–3560.
Maxwell, T. A. and Gifford, A. W.: 1981, *Lunar Planet. Sci.* **XII**, 674–675.
Raitala, J. T.: 1987, *Lunar Planet. Sci.* **XVIII**, 814–815.